

# Memory Effects in Molecular Films of Free-Standing Rod-Shaped Ruthenium Complexes on an Electrode\*\*

Keiichi Terada, Katsuhiko Kanaizuka, Vijay Mahadevan Iyer, Miyabi Sannodo, Sohei Saito, Katsuaki Kobayashi, and Masa-aki Haga\*

Dedicated to Professor Alfred B. P. Lever on the occasion of his 75th birthday

There is significant interest in exploring new information-storage systems for molecule-based devices as an alternative to silicon-based dynamic random access memory (DRAM). The operational principle of a DRAM is based on storing charge on a capacitive metal oxide layer by applying a voltage and reading the charge as a bias current.<sup>[1]</sup> These devices, however, rely on silicon-based technology, in which photolithographic manufacturing is reaching the lower size limit.<sup>[2,3]</sup> Accordingly, as is the case for the development of nanoscale technologies to overcome the fabrication limit of silicon-based devices, molecular electronic devices are an emerging research subject.<sup>[2–5]</sup> The formation of molecular self-assembled monolayers (SAMs) on surfaces is a promising bottom-up approach for the fabrication of molecule-based elements such as switches, memories, and logic gates.<sup>[6–11]</sup> In molecular switches, the injection or exclusion of charges should be activated or controlled by external signals such as electrical or photonic stimuli, and the change of potential gradient should be electrically transduced and transmitted to external circuits.<sup>[9,12–16]</sup> In molecular memories, the charge storage in the molecular layers can be used as a memory bit. Recently, many attempts to construct molecular memory devices have been reported. For example, metalloporphyrins attached chemically onto an electrode stored charges by oxidation or reduction; that is, writing was achieved by oxidation of a porphyrin SAM, and reading was achieved by sensing a current under open-circuit potential after the oxidation.<sup>[17,18]</sup> As another example, the use of successive potential gradients in electron-transfer reactions within a polymer containing both quinone and viologen moieties<sup>[19]</sup> or in bilayer films composed of two polymers, namely,  $[M(\text{phen})_2(\text{vbp})]^{2+}$  (where M is ruthenium or osmium, phen is 1,10-phenanthroline, and vbp is 4-methyl-4'-vinyl-2,2'-bipyridine), made it

possible to trap the charge between layers in the films.<sup>[20]</sup> Furthermore, photogenerated charge storage has been reported in hetero-Langmuir–Blodgett films<sup>[21]</sup> and liquid-crystalline zinc porphyrin, both of which are considered potential candidates for memory devices.<sup>[22]</sup>

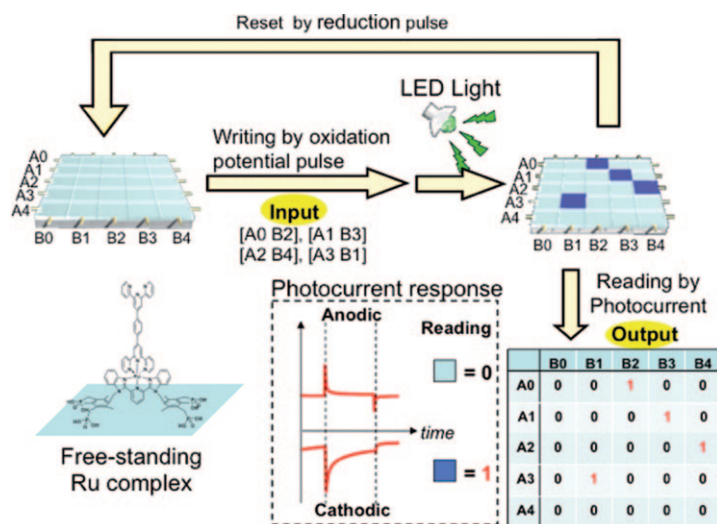
We recently reported immobilization of redox-active ruthenium complexes on an indium tin oxide (ITO) surface and multilayer formation of the redox-active metal complexes by layer-by-layer assembly using zirconium(IV) phosphonate on ITO.<sup>[23–25]</sup> Herein, focusing on the photoelectrochemical response on an ITO electrode, we describe a novel memory effect in rod-shaped ruthenium complexes immobilized at the interface of an electrolyte and a molecular SAM; that is, after a pulse is applied with sufficiently high voltage to oxidize the immobilized ruthenium complex, the original anodic photoresponse is switched to a cathodic one. Our concept for the memory device cells uses this inversion of the photocurrent in the molecular SAM film (Scheme 1). In the writing operation, a pulse voltage which is high enough to oxidize the ruthenium complex is applied to a specific cell address in the SAM array. The reading operation detects the change in the photocurrent under light irradiation. We can read out both “0” and “1” states in the cells by the detection of the direction of the photocurrent. The data can be erased by application of a potential application below 0 V. The operating principle is totally different from that of well-established DRAM and other reported memory devices.

A series of mononuclear, dinuclear, and trinuclear ruthenium complexes (**1–4**, Scheme 2) bearing phosphonate anchors were synthesized. 1,4-Bis(2,2',6',2''-terpyridine-4'-yl)benzene (tpy-ph-tpy) was selected as a bridging ligand, because it is widely used for constructing one-dimensional polynuclear metal complexes.<sup>[26–29]</sup> Surface immobilization of the ruthenium complexes on an ITO electrode was achieved by immersing a bare electrode in a solution of ruthenium complex (50  $\mu\text{M}$ ) in methanol/water (1:1 v/v) for three hours and subsequently washing with methanol and water twice and drying in a nitrogen flow. In particular, the tetrapodal phosphonate anchors in the bis(benzimidazolyl)pyridine ligand (abbreviated LX) kept the molecular orientation vertical to the ITO surface. To prepare complex **3**, a surface self-limiting reaction on immobilized  $[\text{Ru}(\text{LX})(\text{tpy-ph-tpy})]$  (**2**) was applied. Complex **2** immobilized on an ITO electrode was successively immersed in solutions of  $\text{Fe}(\text{BF}_4)_2$  in water and tpy-ph-tpy in chloroform, which afforded the dinuclear ruthenium iron complex  $[(\text{LX})\text{Ru}(\text{tpy-ph-tpy})\text{Fe}(\text{tpy-ph-tpy})]$  (**3**) immobilized on the ITO electrode. The characteristic

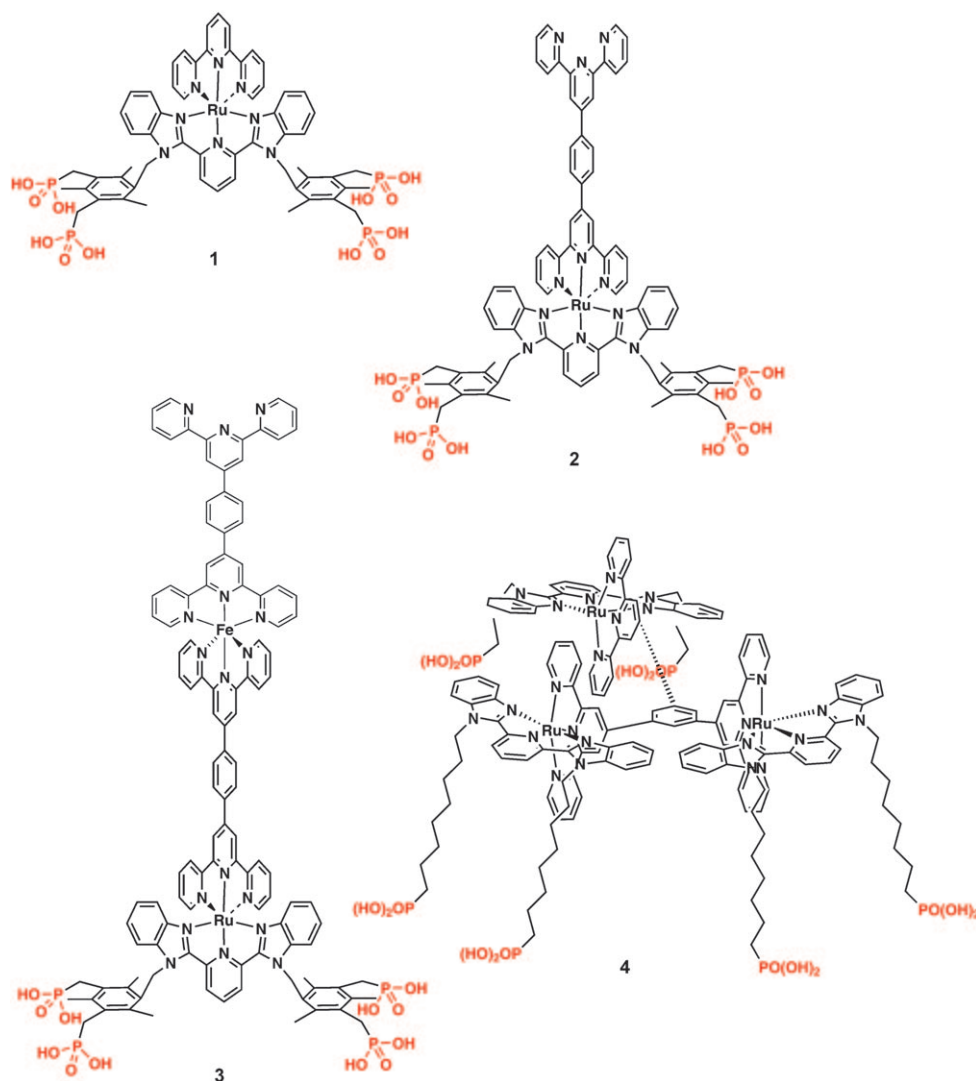
[\*] Dr. K. Terada, Dr. K. Kanaizuka, V. M. Iyer, M. Sannodo, S. Saito, Dr. K. Kobayashi, Prof. M. Haga  
Department of Applied Chemistry, Chuo University  
1-13-27 Kasuga, Bunkyo-ku, Tokyo 112-8551 (Japan)  
Fax: (+81) 3-3817-1908  
E-mail: mhaga@kc.chuo-u.ac.jp  
Homepage: <http://www.chem.chuo-u.ac.jp/~iimc/english/index.html>

[\*\*] This work was supported by the Ministry of Education, Science, Sports, and Culture for a Grant-in-Aid for Priority Area “Coordination Programming” (No. 21108003) and also for Scientific Research (No. 21350082).

Supporting information for this article is available on the WWW under <http://dx.doi.org/10.1002/anie.201100142>.



**Scheme 1.** Operational principle of the memory cells based on redox-active SAM film composed of ruthenium complexes. For memory cells at array crossing points, an applied potential pulse can be read out by detecting the direction of the photocurrent.



**Scheme 2.** Structures of ruthenium complexes 1–4.

UV absorption band at 590 nm corresponding to the  $\text{Fe}^{\text{II}}$ -tpy-ph-tpy metal-to-ligand charge transfer (MLCT) transition (in addition to the  $\text{Ru}^{\text{II}}$ -tpy-ph-tpy MLCT band around 500 nm) was observed, thus indicating the formation of a heterodinuclear ruthenium iron complex. The surface characterization of ruthenium complexes **1** to **3** on the ITO electrode was performed by UV/Vis spectroscopy (Figure S1 in the Supporting Information), cyclic voltammetry (Figure S2 in the Supporting Information), X-ray photoelectron spectroscopy (XPS), and atomic force microscopy (AFM) measurements. Cyclic voltammograms of complexes **1** and **2** showed quasi-reversible one-electron oxidations at +0.76 and +0.78 V, respectively, vs.  $\text{Ag}/\text{AgNO}_3$  (0.01M  $\text{AgNO}_3$  in 0.1M TBABF<sub>4</sub> in  $\text{CH}_3\text{CN}$ , abbreviated as  $\text{Ag}/\text{Ag}^+$ ; TBA = tetrabutylammonium).

Under thin-layer electrochemical conditions for both **1** and **2** immobilized on the ITO electrode (Figure S3 in the Supporting Information), a stable electrochromic response between  $\text{Ru}^{\text{II}}$  and  $\text{Ru}^{\text{III}}$  states was observed (in  $\text{CH}_3\text{CN}/0.1\text{M TBABF}_4$ ). After a

different voltage-pulse sequence was applied to the ruthenium-complex-modified ITO electrode, photocurrent response under light irradiation at 500 nm in  $\text{CH}_3\text{CN}$  was detected without any sacrificial reagents (Figure 1). All of the ruthenium complexes (**1**–**4**) showed an anodic response of the transient photocurrent. Under these conditions, the bare ITO electrode did not show any photocurrent response, as expected. Surprisingly, after a potential pulse between 0 and +1.0 V was applied to the ruthenium-modified electrode, a cathodic transient photocurrent was observed (Figure 1). When the applied amplitude of the voltage pulse was changed from –0.4 to +1.0 V, the current direction changed from anodic to cathodic at around +0.6 V (see Figure S7 in the Supporting Information). As for the erasing operation, the application of a negative voltage pulse between 0 and –1.0 V to the same ruthenium-modified electrode restored the original anodic photocurrent response (see Figure S8 in the Supporting Information).

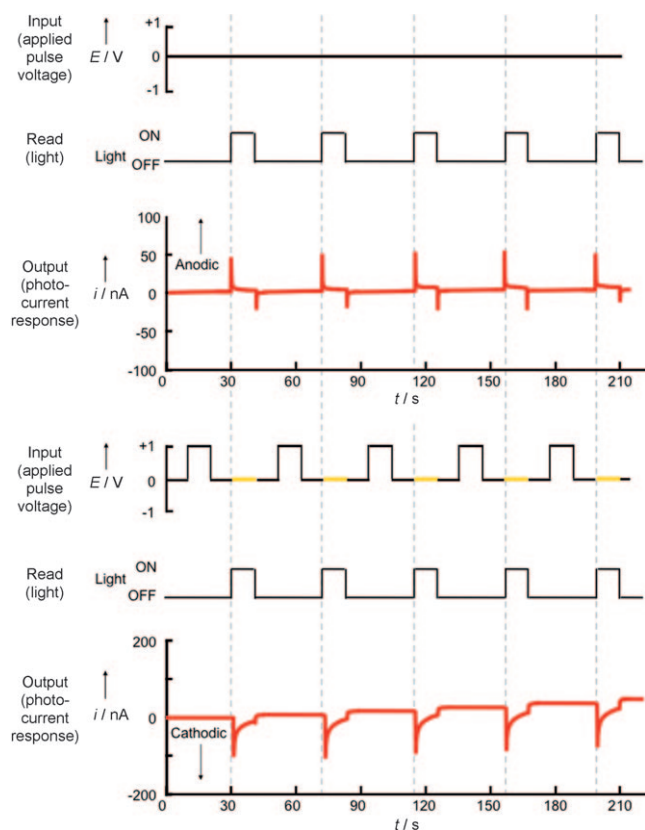


**Figure 1.** Write/read cycle of the SAM of **2** on an ITO electrode in  $\text{CH}_3\text{CN}$  (0.1 M TBABF<sub>4</sub>). The timing of the voltage-pulse input and the light-illumination read operation are shown along with the generated photocurrent-response output.

This photocurrent reversal was only observed when the pulse duration was longer than 0.001 s. The action spectrum of the ruthenium-modified electrode was obtained from the wavelength dependence of the anodic and cathodic photocurrents. The obtained action spectrum is in good agreement with the UV/Vis spectra of complex **2**, thus indicating that the MLCT band is responsible for generating the photocurrent (see Figure S4 in the Supporting Information). In contrast, trinuclear ruthenium complex **4** (Scheme 1) exhibited only anodic transient photocurrent, regardless of whether the voltage pulse had been applied or not. Even when a positive voltage pulse of +1.0 V was applied to oxidize Ru<sup>II</sup> to Ru<sup>III</sup>, only the anodic transient photocurrent was observed (see Figure S5 in the Supporting Information), although the anodic current density became smaller. It is concluded from these results that the photoelectrochemical behavior of the ruthenium-modified ITO electrode meets the basic requirement for the write/read operation of a molecular memory device, that is, writing by a positive voltage pulse above +0.6 V, reading by the cathodic photocurrent response, and erasing by a negative applied potential.

The surface morphology of the modified flat ITO electrode (surface roughness less than 1 nm) was investigated by AFM to clarify the molecular orientation of the ruthenium complexes (see Figure S5 in the Supporting Information). Sparse dots with a pinnacle shape were observed on a low-coverage modified ITO surface. The average molecular

heights for these molecular dots of complexes **1**, **2**, **3**, and **4** on the flat ITO electrode were 1.2, 2.2, 3.7, and 1.2 nm, respectively, which strongly indicates that ruthenium complexes **1**, **2**, and **3** assume an upright molecular orientation on the surface. A similar molecular orientation has been observed in the case of a ruthenium complex with tetrapodal phosphonate anchors and a DNA intercalator site on a mica surface.<sup>[25]</sup> In contrast, complex **4** has a canopied structure with six phosphonate anchor groups, in which the N-Ru-N axis intersecting the octahedral bis(tridentate) ruthenium complex was horizontally aligned, as reported.<sup>[30]</sup> The cathodic photocurrent density increased in the order **1** < **2** < **3**, which is in accord with the increasing order of the molecular height (Figure 2). If the voltage pulse was not applied,

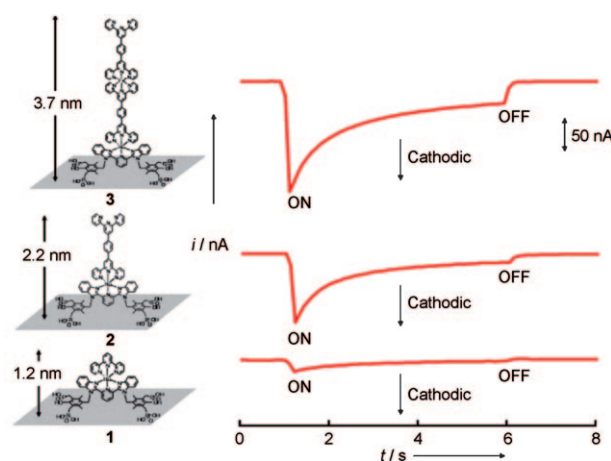


**Figure 2.** Cathodic photocurrent response of ruthenium complexes **1** (bottom), **2** (middle), and **3** (top) on an ITO electrode after the potential pulse was applied. Irradiation at  $\lambda = 500$  nm.

however, the observed anodic photocurrent for complexes **2** and **3** was almost the same magnitude as that for complex **1**. It is concluded that the anodic transient photocurrent derives from the electron injection from the excited state of the ruthenium complex to the ITO electrode without the addition of any sacrificial materials.

Similarly, if the cathodic photocurrent arises from the photoinduced electron transfer, the current should be the same as the anodic one for complex **2** or **3** because of the similar electronic structures of the three complexes with respect to the absorption maxima and oxidation potentials. However, the cathodic current density is dependent on the nature of ruthenium complex. In addition, the cathodic photocurrent density depends on both electrolyte concentration and solvent polarity. Lowering either electrolyte concentration or solvent polarity (by using  $\text{CH}_2\text{Cl}_2$  instead of  $\text{CH}_3\text{CN}$ ) decreases the cathodic current; however, the anodic current stayed almost constant, even when the experimental conditions were changed (see Figure S9 in the Supporting Information). These results indicate that the charge within the electric double layer plays an important role in cathodic photocurrent generation.

The photoelectrochemical behavior of complex **4** is quite distinct from that of complexes **1–3** owing to the molecular

orientation of the immobilized complexes relative to the octahedral N-Ru-N  $C_2$  axis, which is vertical to the surface normal for **1–3** and horizontal for **4**. A significant vertical dipole was induced under the Ru-tpy-ph-tpy MLCT excitation of the ruthenium complexes with upright orientation. On the basis of these results, the photocurrent-inversion behavior of the upright ruthenium complexes can be interpreted as follows: First, for the modified ITO electrode, an anodic transient current was generated by electron injection from the photoexcited ruthenium complexes into the ITO. After the pulsed voltage was applied, a relatively large cathodic transient photocurrent, derived from a non-Faradaic discharge process, was observed. Upon application of a voltage pulse high enough to oxidize  $Ru^{II}$  to  $Ru^{III}$ , anions moved to the ruthenium-modified surface to compensate for the electrochemically generated positive charge, which led to formation of ion pairs. When the applied voltage pulse was switched back to zero,  $Ru^{III}$  rapidly switched back to  $Ru^{II}$ . However, the asymmetric ion partitioning remained for a while. This process stored the charge, depending on the molecular height of the ruthenium complexes, and the ion asymmetry was released by the unidirectional Ru-L MLCT photoexcitation on the surface, the mechanism of which is shown schematically in Figure 3.

To shed light on the charging of the molecular layer, electrochemical impedance spectroscopy (EIS) on the ITO electrode modified with complex **2** was measured (Figure 4). Nyquist plots of EIS show a remarkable change in resistance before and after application of the voltage pulse on the ruthenium-modified electrode. EIS is interpreted by curve fitting of the data to equivalent circuit models, as shown in the inset of Figure 4. The  $R_{ct}$  values (ct = charge transfer) were calculated as 119  $\Omega$  (open dots in Figure 4) and 212  $\Omega$  (inverted triangles) before and after applying the voltage pulse, respectively. At the same time, the defect-site resistance or ion-penetration resistance  $R_d$  was varied from 6.71 to 14.9 k $\Omega$ . The increase of the values of the resistive elements indicates that anions were kept inside the void space of the molecular layer on the ITO electrode and inhibited the electron transfer between ferrocene and the electrode. After photoirradiation, the resistive element  $R_{ct}$  and  $R_d$  values obtained by EIS slowly returned to the original. When the photoresponse of the Ru complex immobilized on the ITO electrode was measured at a certain time lag after the applied pulse, the cathodic photocurrent exponentially decreased with increasing time after the pulse was applied. The half-current period was about 30 min.

In conclusion, in a ruthenium-complex-modified ITO electrode, an anodic transient photocurrent was generated by electron injection from the excited ruthenium complex to the

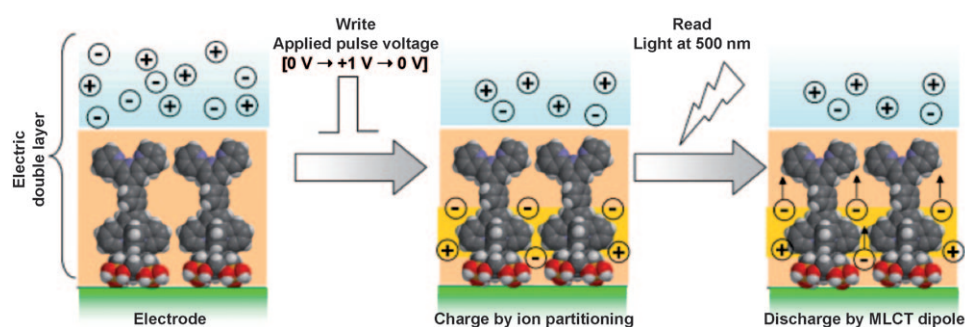


**Figure 3.** Schematic interpretation of ion partitioning for the formation of ion pairs after application of a potential pulse and subsequent ion release by photoirradiation. Anions are stored in the void space around the Ru SAM films. Space-filling depictions of **2** represent the Ru complexes. P yellow, O red, N blue, C gray, H white.

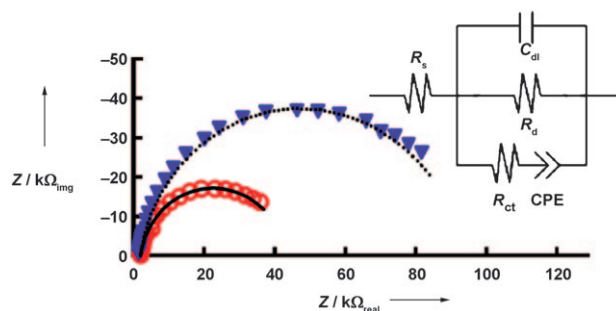


**Figure 4.** EIS of Ru complex **2** immobilized on an ITO electrode together with simulated curves: before voltage-pulse application (open dots); after voltage-pulse application (inverted triangles) in 0.1 M TBABF<sub>4</sub> containing 0.1 mM ferrocene as an electron-transfer probe at an applied potential of +0.3 V vs. Ag/AgNO<sub>3</sub> with 10 mV excitation signal.  $R_s$  = solution resistance,  $C_{dl}$  = double layer capacitance, CPE = constant phase element.

ITO electrode. However, after a pulse of high enough voltage to oxidize  $Ru^{II}$  to  $Ru^{III}$  was applied, the transient photocurrent was reversed; that is, a cathodic current was generated. This photocurrent inversion arises from the participation of a non-Faradaic discharging process that releases anions accompanied by photoexcitation of the immobilized ruthenium complex. The competition between the fast electron transfer (electron injection from the ruthenium complex) and the slow ion movement on the modified ITO electrode is responsible for the photocurrent inversion. Furthermore, both the molecular orientation and the oxidation reaction of the Ru-complex SAM films are prerequisites for the cathodic photocurrent response. This kind of modified electrode has a potential to operate as a memory device. Writing can be achieved by the applied potential pulse, reading by the transient photocurrent, and erasing by a negative potential pulse. This is the first report on a memory device based on surface-immobilized ruthenium complexes with anion storage capability. Although the well-established DRAM cells are operated by an applied voltage and current reading, the present molecular memory device required a voltage pulse, light, and current reading, which is a drawback as an alternative of DRAM cells. Since similar memory effects can be expected for photo- and electrochemi-

cally-active metal–organic frameworks (MOF) on surfaces, new applications, for example as imaging sensors, might be expected. Further investigations aimed at the use of free-standing redox-active complexes as molecular units for the assembly of new MOF structures are underway in our group.

Received: January 7, 2011

Revised: March 9, 2011

Published online: May 30, 2011

**Keywords:** electrochemistry · memory effects · molecular devices · photochemistry · self-assembly

- [1] R. Waser, *Nanoelectronics and Information Technology*, Wiley-VCH, Weinheim, **2003**.
- [2] R. L. Carroll, C. B. Gorman, *Angew. Chem.* **2002**, *114*, 4556–4579; *Angew. Chem. Int. Ed.* **2002**, *41*, 4378–4440.
- [3] Y. Wada, M. Tsukada, M. Fujihira, K. Matsushige, T. Ogawa, M. Haga, S. Tanaka, *Jpn. J. Appl. Phys. Part 1* **2000**, *39*, 3835–3849.
- [4] J. R. Heath, M. A. Ratner, *Phys. Today* **2003**, *56*, 43–49.
- [5] B. Ulgu, H. D. Abruna, *Chem. Rev.* **2008**, *108*, 2721–2736.
- [6] K. Nakazato, H. Ahmed, *Adv. Mater.* **1993**, *5*, 668–671.
- [7] C. G. Joachim, J. K. Aviram, *Nature* **2000**, *408*, 541–548.
- [8] M. Ratner, J. Jortner in *Molecular Electronics: A 'Chemistry for the 21st Century'* (Eds.: J. Jortner, M. Ratner), Blackwell Science, Oxford, **1997**, p. 5.
- [9] a) K. Szaciłowski, W. Macyk, G. Stochel, *J. Am. Chem. Soc.* **2006**, *128*, 4550–4551.
- [10] a) G. de Ruiter, E. Tartakovsky, N. Oded, M. E. van der Boom, *Angew. Chem.* **2010**, *122*, 173–176; *Angew. Chem. Int. Ed.* **2010**, *49*, 169–172; b) J. Lee, H. Chang, S. Kim, G. S. Bang, H. Lee, *Angew. Chem.* **2009**, *121*, 8653–8656; *Angew. Chem. Int. Ed.* **2009**, *48*, 8501–8504; c) A. Bandyopadhyay, S. Sahu, M. Higuchi, *J. Am. Chem. Soc.* **2011**, *133*, 1168–1171.
- [11] M. Amelia, L. Zou, A. Credi, *Coord. Chem. Rev.* **2010**, *254*, 2267–2280.
- [12] J. Matsui, M. Mitsuishi, A. Aoki, T. Miyashita, *Angew. Chem.* **2003**, *115*, 2374–2377; *Angew. Chem. Int. Ed.* **2003**, *42*, 2272–2275.
- [13] H. S. Mandal, I. J. Burgess, H.-B. Kraatz, *Chem. Commun.* **2006**, 4801–4804.
- [14] L. F. O. Furtado, A. D. P. Alexiou, L. Goncalves, H. E. Toma, K. Araki, *Angew. Chem.* **2006**, *118*, 3215–3218; *Angew. Chem. Int. Ed.* **2006**, *45*, 3143–3146.
- [15] S. Nitahara, N. Terasaki, T. Akiyama, S. Yamada, *Thin Solid Films* **2006**, *499*, 354–358.
- [16] S. Gawęda, A. Podborska, W. Macyk, K. Szaciłowski, *Nanoscale* **2009**, *1*, 299–316.
- [17] K. M. Roth, N. Dontha, R. B. Dabke, D. T. Gryko, C. Clausen, J. S. Lindsey, D. F. Bocian, W. G. Kuhr, *J. Vac. Sci. Technol. B* **2000**, *18*, 2359–2364.
- [18] K. M. Roth, J. S. Lindsey, D. F. Bocian, W. G. Kuhr, *Langmuir* **2002**, *18*, 4030–4040.
- [19] G. T. R. Palmore, D. K. Smith, M. S. Wrighton, *J. Phys. Chem. B* **1997**, *101*, 2437–2450.
- [20] P. G. Pickup, R. W. Murray, *J. Am. Chem. Soc.* **1983**, *105*, 4510–4510.
- [21] K. Naito, A. Miura, *J. Am. Chem. Soc.* **1993**, *115*, 5185–5192.
- [22] C.-y. Liu, H.-l. Pan, M. A. Fox, A. J. Bard, *Chem. Mater.* **1997**, *9*, 1422–1429.
- [23] M. Haga, K. Kobayashi, K. Terada, *Coord. Chem. Rev.* **2007**, *251*, 2688–2701.
- [24] K. Kobayashi, N. Tonegawa, S. Fujii, J. Hikida, H. Nozoye, K. Tsutsui, Y. Wada, M. Chikira, M. Haga, *Langmuir* **2008**, *24*, 13203–13211.
- [25] G. Cao, H.-G. Hong, T. E. Mallouk, *Acc. Chem. Res.* **1992**, *25*, 420–427.
- [26] Y. Nishimori, K. Kanaizuka, T. Kurita, T. Nagatsu, Y. Segawa, F. Toshimitsu, S. Muratsugu, M. Utsuno, S. Kume, M. Murata, H. Nishihara, *Chem. Asian J.* **2009**, *4*, 1361–1367.
- [27] T. Kurita, Y. Nishimori, F. Toshimitsu, S. Muratsugu, S. Kume, H. Nishihara, *J. Am. Chem. Soc.* **2010**, *132*, 4524–4525.
- [28] N. Tuccitto, V. Ferri, M. Cavazzini, S. Quici, G. Zhavnerko, A. Licciardello, M. A. Rampi, *Nat. Mater.* **2009**, *8*, 41–46.
- [29] Y. Liang, R. H. Schmehl, *J. Chem. Soc. Chem. Commun.* **1995**, 1007–1008.
- [30] K. Terada, K. Kobayashi, M. Haga, *Dalton Trans.* **2008**, 4846–4854.